Organic & Biomolecular Chemistry

ROYAL SOCIETY OF CHEMISTRY

PAPER

View Article Online
View Journal | View Issue

Cite this: *Org. Biomol. Chem.*, 2024, **22**, 5314

Visible-light promoted oxidative annulation of 2-naphthols with phenylglyoxal monohydrates toward hydroxy-naphthofuranone and its derivatives†

Vijayakumar Hemamalini,[a] Markabandhu Shanthi,[a] Bhaskaran Shankar,[c] Rambabu Dandela,[b] Karuppaiah Perumal[a] and Subburethinam Ramesh *[a]

Received 29th April 2024,
Accepted 6th June 2024

DOI: 10.1039/d4ob00693c

rsc.li/obc

A highly efficient and innovative method involving base-mediated oxidative annulation between 2-naphthols and phenylglyoxal monohydrate under visible light irradiation has been successfully developed. This method leads to the formation of oxygen-containing heterocyclic compounds, particularly hydroxy-naphthofuranone derivatives, encompassing a unique quaternary carbon center. An X-ray diffraction study has unambiguously confirmed the structure of one such derivative. In particular, water molecules in this reaction serve various functions as a solvent, reagent, and additive, with the conversion of the process found to be influenced by the volume of water present. This atom-economical approach demonstrates tolerance for different substituents in both phenylglyoxal monohydrate and 2-naphthol, enabling the synthesis of a variety of naphthofuranones in satisfactory to good yields. The formation of a naphthofuranium cationic intermediate under acidic circumstances enables the formation of C–C or C–O bonds with a wide range of aromatic or alcoholic nucleophilic partners. Furthermore, the identification and generation of pinacol-type starting precursors from these naphthofuranone derivatives enable the synthesis of highly regioselective naphthofuran derivatives.

Introduction

A range of biologically active compounds containing a furanone structure have been identified, displaying a diverse array of biological activities.[1] These oxygen-containing heterocyclic compounds are classified based on the position of the oxygen atom and the carbonyl group, falling into three categories: 3(2*H*)-furanone, 2(5*H*)-furanone, and 2(3*H*)-furanone.[2] Found in numerous natural products and biologically active substances, 3(2*H*)-furanone derivatives demonstrate various activities, including anti-tuberculosis, antioxidant, analgesic, antiulcer, anticonvulsant, anticancer, antibacterial, antifungal, and anti-inflammatory properties (Fig. 1, **1–5**).[3] Naphthofuranone, furanone and naphthalene-fused structures, found not only in secondary metabolites but also in their derivatives, exhibit significant biological activities. Moreover, several fused furan derivatives, naphthofurans and benzofurans in particular, are widely known for their remarkable biological properties and presence in natural products.[4] Almost thirty medications containing benzofuran have been approved by the US Food and Drug Administration (USFDA).[5] Furthermore, naphthofurans have recently received a lot of attention due to their potential efficacy in the design and synthesis of therapeutics for cancer treatment,[6] Alzheimer's disease inhibitors,[7] modulators of human protein kinase,[8] and nuclear receptors,[9] and a variety of other biological activities[10] (Fig. 1, **6–9**).

It was hypothesised that **10a**, an alpha hydroxy naphthofuranone molecule, would be an appropriate precursor for functionalization as it can easily eliminate a water molecule in the presence of an acid and would generate naphtho[2,1-*b*]furan-3-ium **11a** intermediate. Furthermore, electrophilic substitution reactions using various aromatic and aliphatic nucleophiles can be performed on the *in situ* generated naphtho[2,1-*b*]furan-3-ium carbocation **11a** for the preparation of functionalized naphthofuranone **12a**. When reduced, the

[a]*Department of Chemistry, School of Chemical and Biotechnology, SASTRA Deemed University, Thanjavur 613 401, Tamil Nadu, India. E-mail: rameshsbdu@gmail.com*
[b]*Department of Industrial and Engineering Chemistry, Institute of Chemical Technology, Indian Oil Odisha Campus, Samantapuri, Bhubaneswar, Odisha 751013, India*
[c]*Department of Chemistry, Thiagarajar College of Engineering, Madurai 625 015, Tamil Nadu, India*

†Electronic supplementary information (ESI) available: Crystal information for **10a**, **21a** and **14g**, general procedure, NMR data and ^{1}H, ^{13}C and HRMS analysis reports. CCDC 2350169, 2350170 and 2360763. For ESI and crystallographic data in CIF or other electronic format see DOI: https://doi.org/10.1039/d4ob00693c

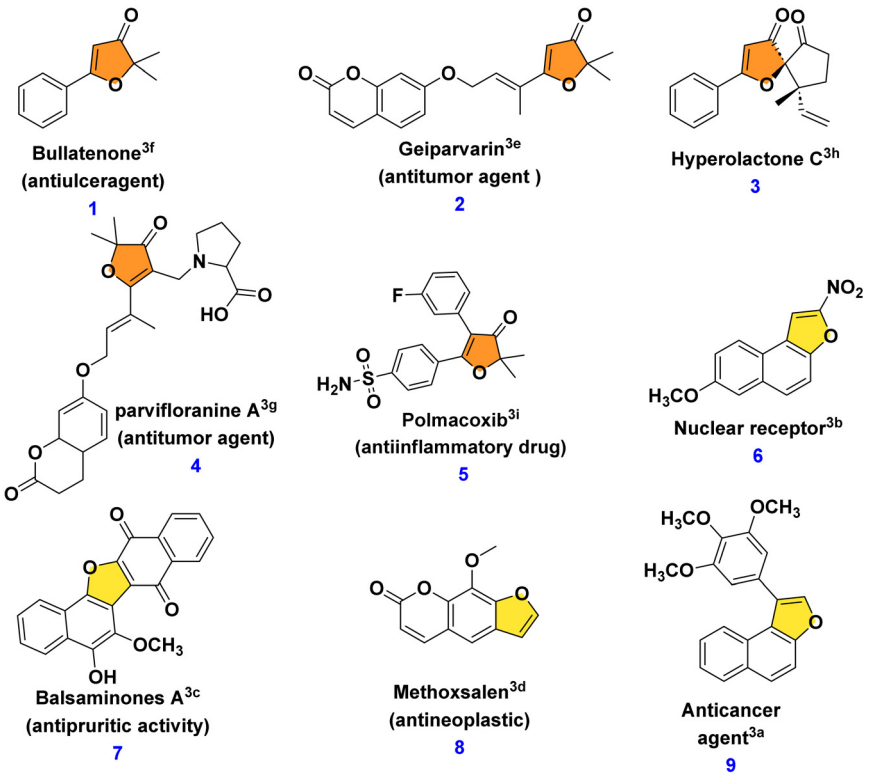

Fig. 1 Examples of bioactive molecules containing furanone and naphthofurans.

alpha-functionalized naphthofuranone **12a** yields naphthofuranol **13a**, which is classified as a pinacol-type precursor. Subsequently, the pinacol-type precursor **13a** would be subjected to an acidic rearrangement reaction, which would produce a regioselective naphthofuran derivative denoted as **14a**. The presence of a furan oxygen atom was expected to be the main driving force for this rearrangement (Scheme 1).

In this context, our goal was to synthesize hydroxy-naphthofuranone **10** and then convert it into naphthofuran **14**. However, the synthesis of hydroxy-naphthofuranone remains highly limited, with no literature reports for its conversion into naphthofuran **14**. Ahmed *et al.*[11] described a microwave-assisted approach for synthesising hydroxy-naphthofuranone **10a** using copper salts under microwave conditions (eqn (a), Scheme 2). Anxin Wu *et al.*[12] recently described the selective oxidative coupling of 2-naphthol (**15a**) and methyl ketone **17a** under iodine/DMSO oxidative conditions (eqn (b), Scheme 2), a method also explored by Chun Cai *et al.*[13] utilizing a copper catalyst (eqn (b), Scheme 2). In addition, Meng-Yang Chang *et al.*[14] developed a unique method for synthesizing naphthofuranone derivative **20** by light and iodine-mediated dearylacetylative dimerization (eqn (c), Scheme 2). However, these methods have several disadvantages, such as high temperatures, dependence on metal catalysts, and limited possibilities for further synthetic modifications of the furanone molecules. We intended to use a metal-free organophotocatalyst triggered by visible light[15] to synthesize hydroxy-naphthofuranones, which would then be used to synthesize different naphthofuranone and naphthofuran derivatives. To the best of our knowledge, there are no reports on the synthesis of naphthofuran from naphthofuranone. The reported methodologies for

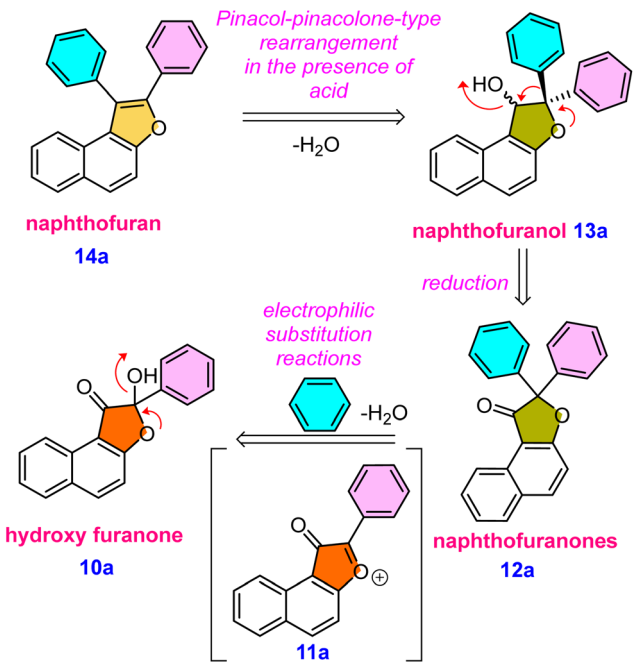

Scheme 1 Retrosynthetic analysis of the synthesis of naphthofuran **14a** from hydroxy-naphthofuranone **10a**.

naphthofuran synthesis rely primarily on metal-mediated C–H activation. The most often used technique involves cyclizing prefunctionalized naphthols, such as 2-alkenyl naphthol, which is typically aided by the addition of a transition metal catalyst.[16] Many methods have been described for preparing these scaffolds *via* base-promoted cyclizations, Lewis or Brønsted acid catalysis, or transition metal catalysis.[17] Here, we demonstrate our unique collective strategies for coupling

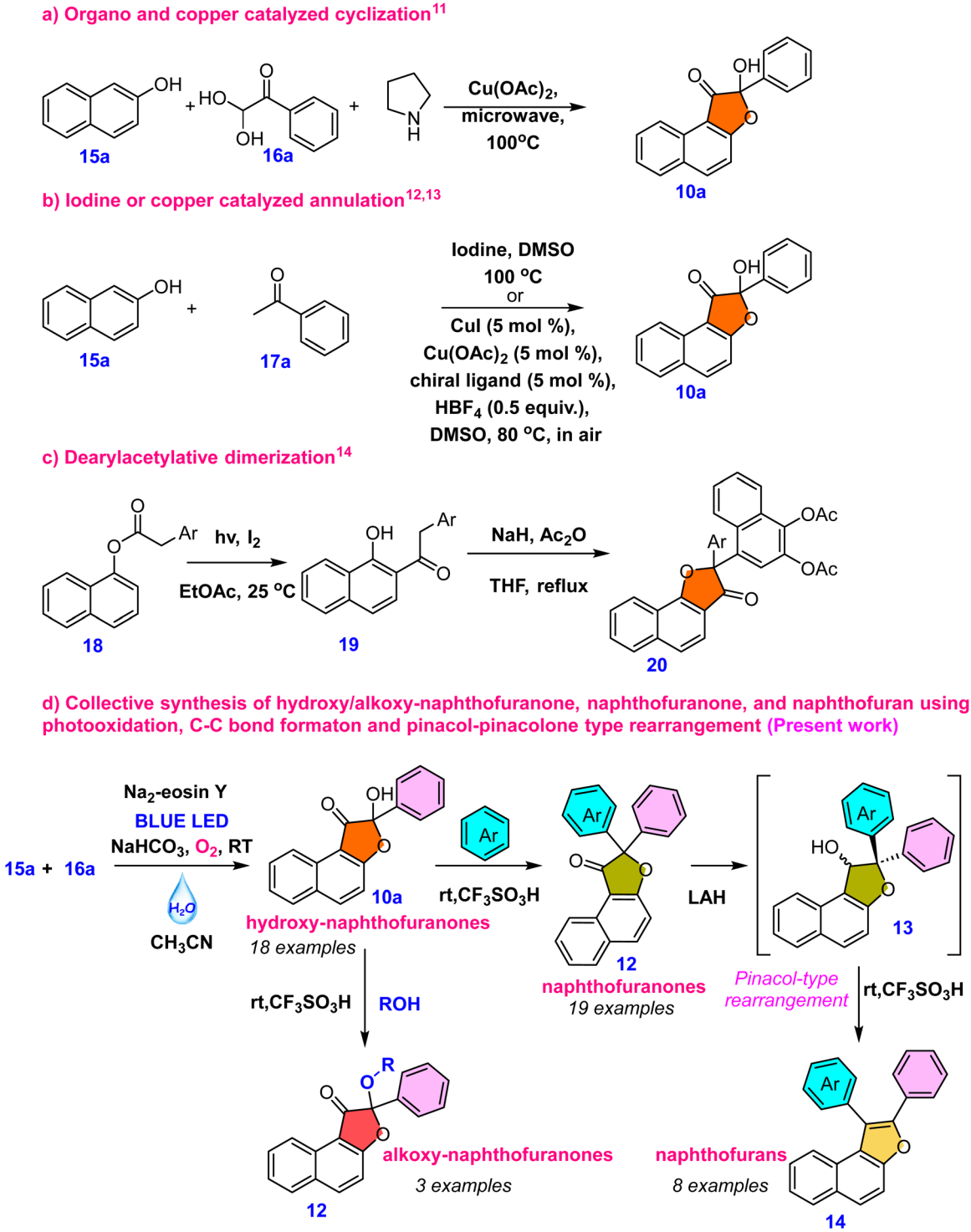

Scheme 2 Various synthetic approaches for the synthesis of hydroxy-naphthofuranone and our synthetic plan for various naphthofuranone and furan derivatives.

2-naphthol **15a** and phenylglyoxal monohydrate **16a** under visible light irradiation to yield a wide range of hydroxy-naphthofuranones **10a–10s** and subsequent modification for the synthesis of naphthofuranone **12a–12s**, alkoxy-naphthofuranone **12t–12v** and naphthofuran derivatives **14a–14h** (eqn (d), Scheme 2).

Initially, 3 W blue LED light was used to optimize the reaction between 2-naphthol **15a** and phenylglyoxal monohydrate **16a** in acetonitrile solvent with a mild base and Na_2–eosin Y under a nitrogen atmosphere (entry 1, Table 1). This resulted in 20% yield of naphtho-3(2*H*)-furanone **10a**, which has a unique quaternary center. Single crystal X-ray analysis and ^1H & ^{13}C NMR spectroscopic studies provided unambiguous confirmation of product **10a**'s structure.[20] The ORTEP structure of **10a** is provided in Table 1. In order to facilitate the solubility of the inorganic base, we next added water (14 equiv.) to the reaction mass and found that the yield of **10a** improved to 35% (entry 2, Table 1). The requirement of base for this reaction was found out from entry 3 as no product **10a** formed in the absence of base (entry 3, Table 1). Consequently, further reactions proceeded in the presence of a base and an additive. As expected, when the reaction was performed under an oxygen atmosphere, the yield of **10a** was improved (entry 4, Table 1). To emphasize the crucial role of water as an additive, further optimization reactions were focused on water equivalents (entries 5–7, Table 1). These experiments led to the conclusion that the presence of 50 equivalents of water in acetonitrile solvent favored the desired product with a 81% yield (entry 6, Table 1). Later optimization studies concentrated on trying out several solvents, including DMSO, DMF, ethanol, and methanol; acetonitrile gave the maximum yield of the product (entries 6 and 8–11, Table 1). Next, we concentrated on examining the effect of other bases on our reaction, such as NaOH, Na_2CO_3, and K_2CO_3. Among these, $NaHCO_3$ appeared to be the superior base compared to others (entries 6 and 12–14, Table 1). Subsequently, we screened various photocatalysts, but observed no enhancement in the product yield (entries 6 and 15–17, Table 1). Different light sources were also

Table 1 Optimization of the reaction conditions

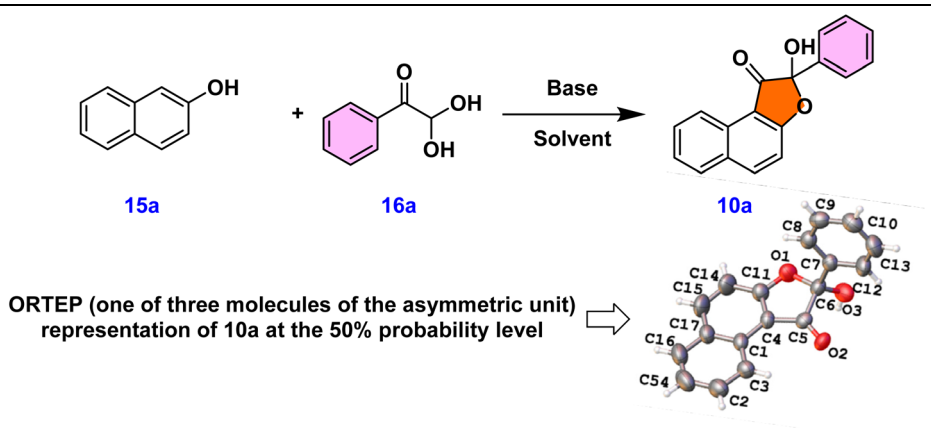

Entry	Base	Solvent	Additive	Catalyst	Conditions	Atm	Yield[a] (%)
1	$NaHCO_3$	ACN	—	Na_2–eosin Y	Blue light	N_2	20
2	$NaHCO_3$	ACN	H_2O (14 equiv.)	Na_2–eosin Y	Blue light	N_2	35
3	—	ACN	H_2O (14 equiv.)	Na_2–eosin Y	Blue light	N_2	ND
4	$NaHCO_3$	ACN	H_2O (14 equiv.)	Na_2–eosin Y	Blue light	O_2	61
5	$NaHCO_3$	ACN	H_2O (30 equiv.)	Na_2–eosin Y	Blue light	O_2	71
6	**$NaHCO_3$**	**ACN**	**H_2O (50 equiv.)**	**Na_2–eosin Y**	**Blue light**	**O_2**	**81**
7	$NaHCO_3$	—	H_2O (70 equiv.)	Na_2–eosin Y	Blue light	O_2	39
8	$NaHCO_3$	Ethanol	H_2O (50 equiv.)	Na_2–eosin Y	Blue light	O_2	63
9	$NaHCO_3$	Methanol	H_2O (50 equiv.)	Na_2–eosin Y	Blue light	O_2	66
10	$NaHCO_3$	DMF	H_2O (50 equiv.)	Na_2–eosin Y	Blue light	O_2	54
11	$NaHCO_3$	DMSO	H_2O (50 equiv.)	Na_2–eosin Y	Blue light	O_2	51
12	NaOH	ACN	H_2O (50 equiv.)	Na_2–eosin Y	Blue light	O_2	53
13	Na_2CO_3	ACN	H_2O (50 equiv.)	Na_2–eosin Y	Blue light	O_2	61
14	K_2CO_3	ACN	H_2O (50 equiv.)	Na_2–eosin Y	Blue light	O_2	59
15	$NaHCO_3$	ACN	H_2O (50 equiv.)	Eosin-Y	Blue light	O_2	81
16	$NaHCO_3$	ACN	H_2O (50 equiv.)	Rose bengal	Blue light	O_2	73
17	$NaHCO_3$	ACN	H_2O (50 equiv.)	Rhodamine B	Blue light	O_2	73.5
18	$NaHCO_3$	ACN	H_2O (50 equiv.)	Na_2–eosin Y	Pink light	O_2	60
19	$NaHCO_3$	ACN	H_2O (50 equiv.)	Na_2–eosin Y	Green light	O_2	51

[a] Isolated yield; reaction conditions: 0.5 mmol of **15a**, 0.6 mmol of **16a**, 0.5 mmol of $NaHCO_3$, 10 mol% of Na_2–eosin Y, 25 mmol of H_2O and acetonitrile as a solvent (0.5 mL) in O_2 atm under a 3 W blue LED.

assessed, emphasizing the importance of blue LED illumination (entries 6, 18 and 19, Table 1).

These results indicated that the reaction between **15a** and **16a** in the presence of $NaHCO_3$ base, with water as an additive, in an oxygen environment under 3 W blue LED light, and with Na_2–eosin Y photocatalyst were the optimum conditions for the formation of the hydroxy-naphthofuranone product **10a** (entry 6, Table 1).

Having established the standard reaction conditions as outlined in entry 6 of Table 1, our next objective was to examine the substrate scope of the reactions employing derivatives of phenylglyoxal monohydrate **16a–16o** and 2-naphthol **15a–15e**, as depicted in Scheme 3. All derivatives of 2-naphthol and phenyl glyoxal monohydrates converted into the corresponding products **10b–10s**, as anticipated, with good results. The introduction of halogen substituents on the phenyl ring of phenyl glyoxal monohydrates, such as 4-F, 4-Cl, and 4-Br, caused decreased yields of products **10b–10d** in comparison with that of **10a**. On the other hand, a 52% lowering of yield was determined when phenyl glyoxal monohydrate's phenyl ring had electron-withdrawing groups such as $-NO_2$ (**10e**). Similarly, the yield of product **10f** decreased by 69% when a 4-CF_3 group was incorporated into the phenylglyoxal moiety. When 2,4-dichloro substituents were present on phenyl glyoxal monohydrate, a moderate yield of **10i** (77%) was produced. However, oxoaldehyde substituted with electron-donating groups such as 4-CH_3 and 4-OCH_3 gave the desired product in better yields of 68% (**10g**) and 69% (**10h**), respectively. The presence of electron-donating or electron-withdrawing groups did not appear to have a significant impact on the yield. A study into steric effects through *ortho*-chloro and *ortho*-methyl substitution of phenylglyoxal revealed minimal hindrance, providing 73% (**10k**) and 81% (**10l**) yields, respectively. The introduction of a methoxy group at the *meta*-position of the phenyl ring resulted in a yield of 69% for **10j**. Additionally, the reaction utilizing heterocyclic glyoxal derivatives **16m** and **16n** provided products **10m** and **10r** with a moderate yield of 69% and 73%, respectively. Then, 2-naphthyl oxoaldehyde subsequently provided the desired product **10s** with a yield of 70%. The scope of the reaction was then investigated using other 2-naphthol derivatives. When 2-naphthol was substituted with 7-OCH_3, the yield of **10o** enhanced to 81%. 2-Naphthol derivatives substituted with bromo, including 3-bromo and 6-bromo-2-naphthol compounds, provided yields of 77% and 56% for **10q** and **10n**,

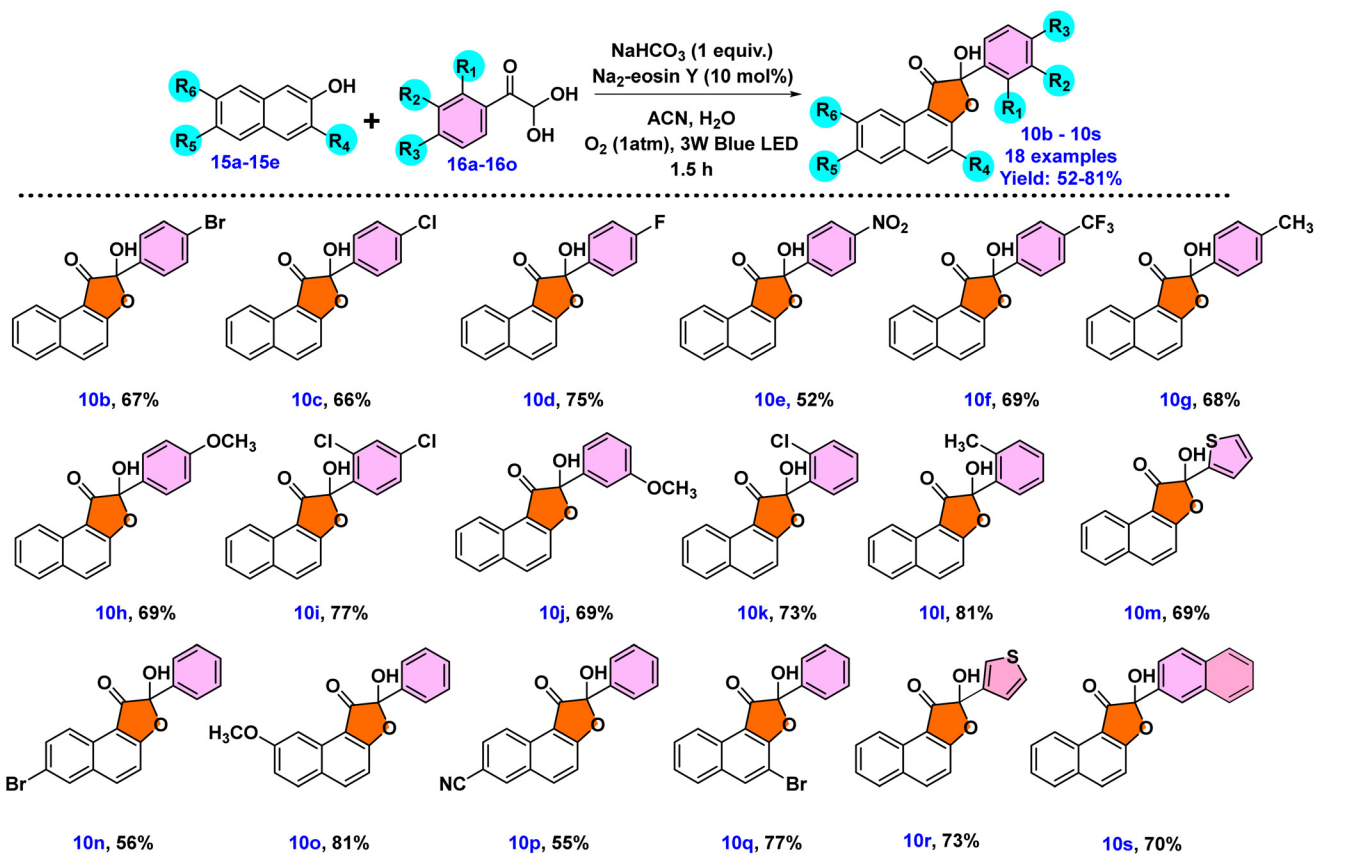

Scheme 3 Substrate scope for the synthesis of hydroxy-naphthofuranone derivatives **10b–10s** using phenylglyoxal monohydrates **16a–16o** and 2-naphthols **15a–15e**. Reaction conditions: 0.5 mmol of **15a**, 0.6 mmol of **16a**, 0.5 mmol of $NaHCO_3$, 10 mol% of Na_2–eosin Y, 25 mmol of H_2O and acetonitrile as a solvent (0.5 mL) in O_2 atm under a 3 W blue LED.

respectively. For 2-naphthol, the inclusion of a 6-CN substituent delivered **10p** with a 55% yield. It is noteworthy that the presence of a cyano group was not tolerated under the conditions reported in the literature.[12] This finding is most likely explained by the stability of –CN in such circumstances or by an insufficient activation of the naphthol derivative with an electron-withdrawing –CN group.

Investigating the synthesis of naphthofuranones **12a–12v** from hydroxy-naphthofuranone derivatives **10** was our next objective. Because the hydroxyl group in **10a** is a poor leaving group due to the formation of a strong conjugate base, we hypothesized that protonation of this hydroxyl group with acid would generate a hydronium ion, a much better leaving group. The hydroxyl group was protonated and a water molecule was eliminated, as expected when triflic acid was used as the acid source. Consequently, the electrophilic substituted product **12b** was obtained in 73% yield by utilizing the *in situ* formed furanium cation **11a** with a xylene molecule. Afterward, we adopted the same strategy to synthesize several naphthofuranone derivatives, **12a**, **12c–12v**. We attained yields ranging from 55% to 98% by employing triflic acid along with appropriate aromatic/alcoholic nucleophilic partners (Scheme 4). *p*-Xylene facilitated the synthesis of several naphthofuranone derivatives **12c–12h** when employing different hydroxy-naphthofuranone derivatives. Notably, the presence of a methoxy group in compound **12f** decreased the yield to 67% compared to those of compounds **12c–12e** and **12g–12h**, probably due to the methoxy group stabilizing the *in situ* formed furanium cation.

On the other hand, we found slower reactivity than for xylene when benzene was used as the nucleophilic partner for the synthesis of **12a**, **12i–12n**. Because benzene is less nucleophilic than xylene, the reaction necessitated slightly higher temperatures to produce compounds **12a**, **12i–12n** in good to outstanding yields. We then investigated some other aromatic nucleophiles, leading to predicted compounds **12o–12s** in a very selective manner. Likewise employing different alcohol derivatives, we effectively produced alkoxy naphthofuranones **12t–12v** under acidic conditions, as shown in Scheme 4.

Our hypothesis aimed to reduce the keto functionality in **12i** to yield the pinacol-type precursor **13b**, followed by an acid-catalyzed rearrangement to produce naphthofuran derivative **14b**. To test this hypothesis, we first reduced compound **12i** using LAH, resulting in a mixture of diastereomeric alcohols **13b** with a dr ratio of 1 : 1 as measured by ^{1}H NMR spectroscopy. Following a simple workup, the diastereomeric mixture **13b** underwent further acid-catalyzed rearrangement. As predicted, the naphthofuran derivative **14b** was produced *via* a smooth rearrangement of the pinacol-type precursor **13b**, giving 95% yield with high regioselectivity (Scheme 5). Electronic effects provide a rationale for the migration of the 4-methyl substituted phenyl ring over the phenyl ring to the electron-deficient carbon.

More specifically, the carbocation would be stabilized more successfully by the +I activity of the methyl-substituted phenyl ring than by the phenyl ring alone. Furthermore, investigation of this type of rearrangement was done on the bromo- and methoxy-substituted groups on the naphthalene core in naphthofuranones **12l–12n**. Following the reduction step, the alcoholic compounds yielded reasonable to outstanding yields of the respective naphthofuran derivatives **14d–14f** under acidic conditions. These findings support two essential insights: first, the generation of a carbocation because of only one product, and second, the prioritization of migration of a more nucleophilic aromatic partner. Compound **12b** upon reduction and then treatment with acid gives **14g**, with the migration of the benzene ring instead of the *p*-xylene group,

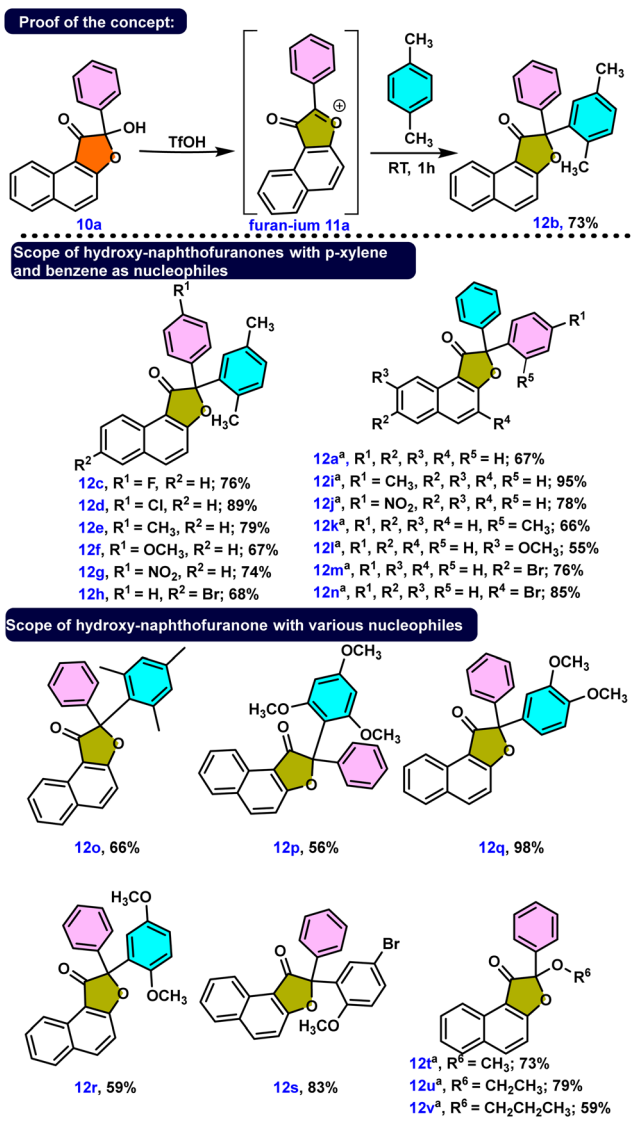

Scheme 4 (a) Proof of concept and (b) synthesis of naphthofuranones **12a–12v** by using various hydroxy-naphthofuranone derivatives along with various nucleophiles. Unless otherwise noted: reaction conditions: 0.5 mmol of **10a**, 1 mmol of nucleophile and 0.5 mmol of triflic acid in a closed reaction vial at room temperature. [a] Reaction temperature is 70 °C.

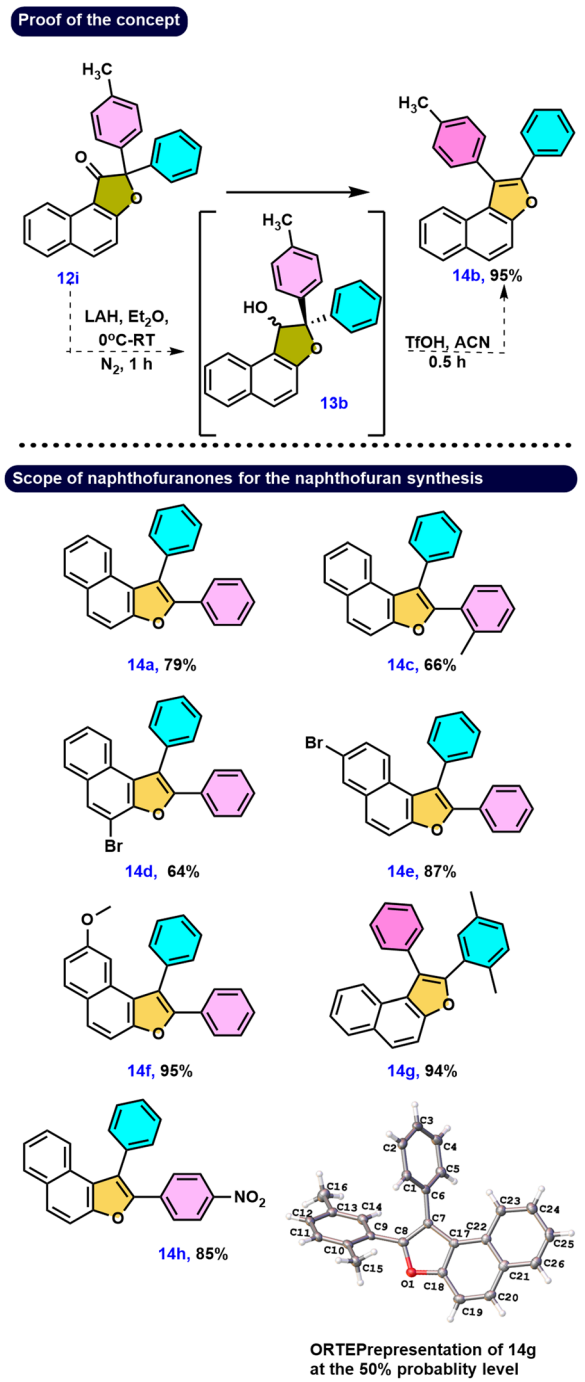

Scheme 5 Synthesis of naphthofurans **14a–14h** using various naphthofuranone derivatives **12a**, **12b**, **12i–12n**. Reaction conditions: 0.5 mmol of **12a**, 1.25 mmol of LAH, and ether as a solvent (0.5 mL) at 0 °C in N_2 atm, then 0.5 mmol of **13a**, 0.5 mmol of triflic acid, and acetonitrile (0.5 mL) as a solvent.

and the regioselectivity of the compound **14g** structure was unambiguously confirmed by single crystal XRD.[20] The ORTEP structure of **14g** is provided in Scheme 5. Similarly, compound **12j**, as predicted, underwent a reduction reaction, and treatment with acid generated only one naphthofuran **14h**, with migration taking place toward the benzene partner instead of the nitroaryl group. The strongly electron-withdrawing $-NO_2$ group is probably responsible for this behavior since it might not be able to stabilize the carbocation enough. Compound **12k**, which included benzene and *ortho*-substituted benzene, was reduced/rearranged to provide compound **14c** with excellent regioselectivity. Here, the phenyl-migrated compound **14c** is produced in excellent yield due to the predominance of steric factors.

Control experiments were then carried out to provide insight into the possible reaction path. Under standard conditions, the reaction between 2-naphthol **15a** and phenylglyoxal monohydrate **16a** was carried out without light or a catalyst. This, as expected, resulted in a decrease in the product yield, highlighting the need for light and a photocatalyst (eqn (1), Scheme 6). Furthermore, the reaction did not proceed under standard conditions in the absence of a base, emphasizing the necessity of a base (eqn (2), Scheme 6). Intriguingly, under standard conditions and in the absence of water, our desired product was generated in a low yield of 20% (eqn (3), Scheme 6). To further understand the role that oxygen plays in the process, more control tests were conducted. As a result, the experiment was carried out under a nitrogen atmosphere rather than an oxygen atmosphere using standard conditions, which led to a lower product yield and illustrated the need for oxygen (eqn (4), Scheme 6). The reactive intermediate **21a** was subsequently isolated, and its structure was confirmed using single XRD[20] and HRMS techniques to deduce the mechanism (eqn (6), Scheme 6). The expected product **10a** was obtained by subjecting the isolated intermediate **21a** to standard reaction conditions (eqn (7), Scheme 6). Scheme 7 elaborates on a plausible mechanism by putting together information from the relevant literature[18] and control experiment results.

Based on the control experiments and various substrate scope in each stage, a possible mechanism is proposed in Scheme 7. The compounds **15a** and **16a** reacted together and produced an intermediate **I** under basic conditions. The intermediate **I** eliminates water and generates an intermediate **II**. The existence of this intermediate emphasizes the vital importance of water. Water can be added to promote the generation of the hydrated intermediate **21a** or **II**. High-resolution mass spectrometry and single XRD analysis confirm the structure of the intermediate **21a**.[20] The ORTEP structure of **21a** is provided in Scheme 6. The organic dye Na_2–eosin Y is excited when visible light is absorbed, and this energy is then transferred to ground-state triplet oxygen species ($^3O_2$). The excited state of the photocatalyst returns to its ground state (Na_2–eosin Y) because of this energy transfer, and triplet oxygen changes into singlet oxygen ($^1O_2$).[19] The reactive intermediate undergoes a hydrogen atom transfer process facilitated by photoactivated oxygen species, providing hydroxyl radical species **III** and hydroperoxyl radical species. These intermediates can be converted into compound **IV** by an insertion reaction. In the end, the desired product **10a** is formed by an intramolecular cycliza-

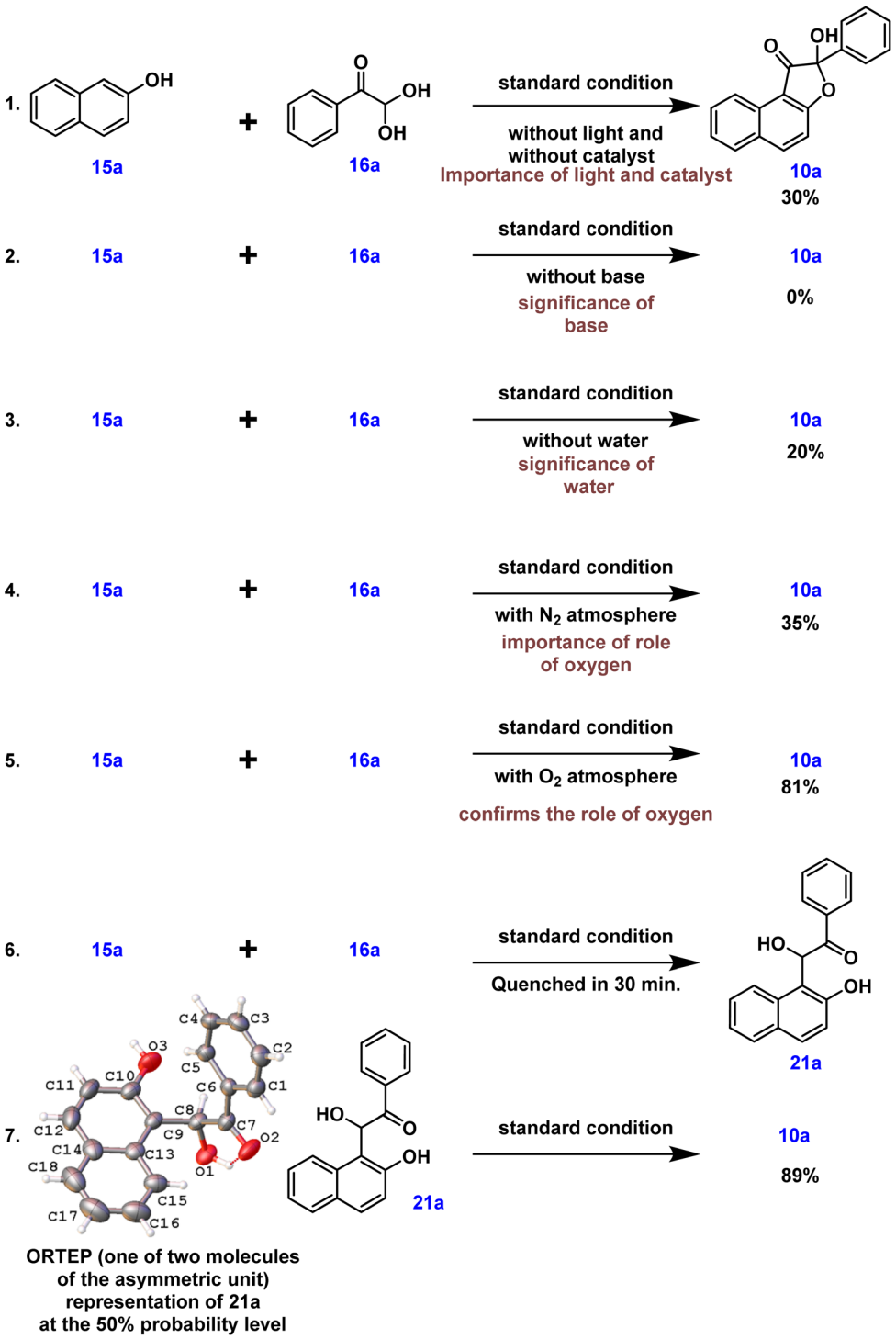

Scheme 6 Control experiments.

tion that occurs when the oxygen atom attacks the β-carbonyl group present in the intermediate **V**. Surprisingly, protonation of –OH happens under acidic circumstances, causing the lone pair of oxygen to induce electron movement and eliminate a water molecule. The resultant furanium **11a** ion is unstable, but it is possible to regenerate the single oxygen atom by inserting incoming nucleophiles. Naphthofuranone **12a** is further reduced to yield the pinacol-type precursor **13a**, which is then subjected to an acid-catalyzed pinacol-type rearrangement reaction to produce the furan derivative **14a** *via* transition intermediates **13a′** and **13a″** (Scheme 7).

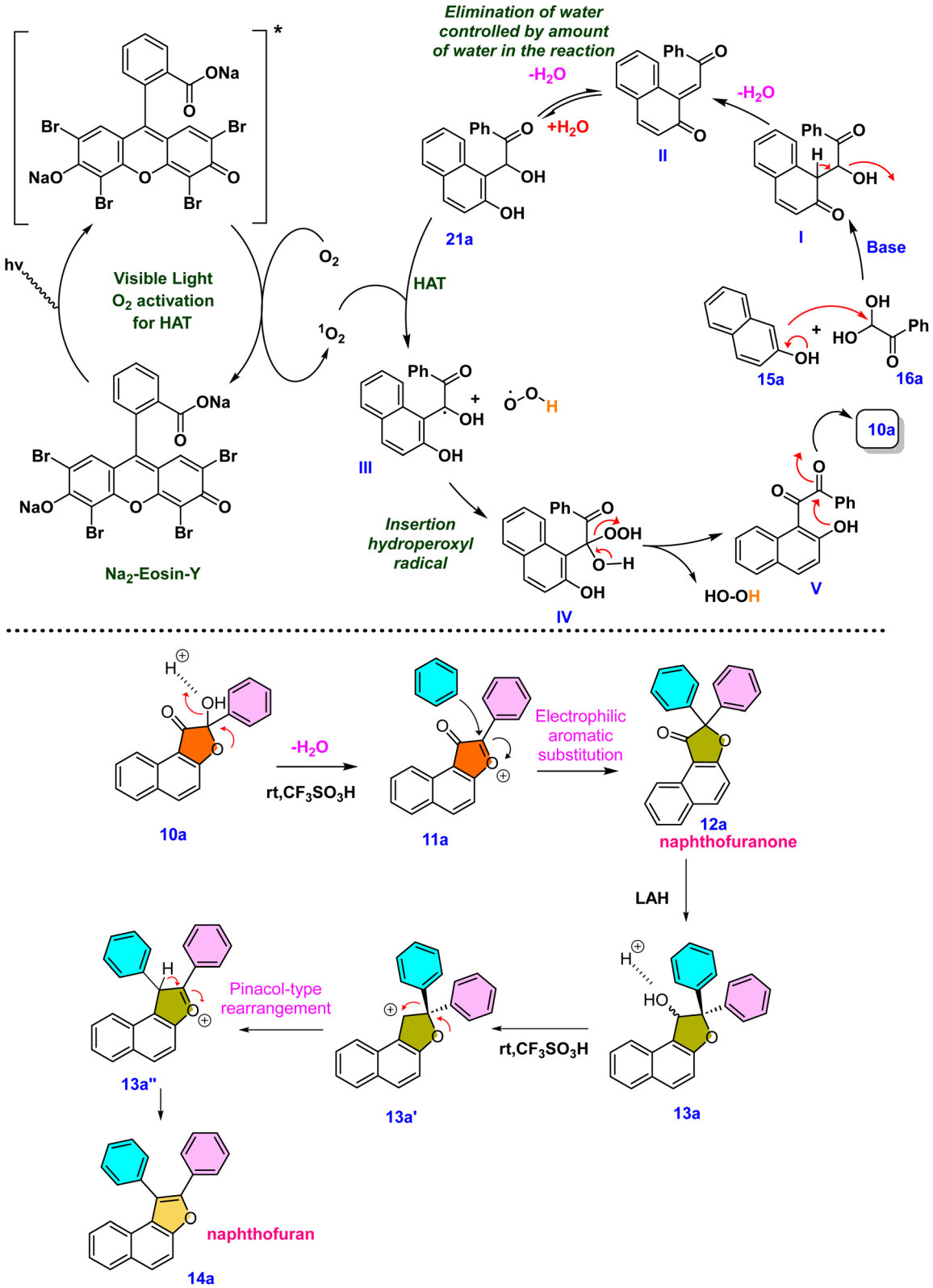

Scheme 7 Plausible mechanism.

Conclusion

In conclusion, this work highlights a unique approach for synthesizing hydroxy-naphthofuranone using visible light irradiation. Water functions as both a reagent and an additive, playing an important role in the process. Furthermore, our approach was effective in synthesising naphthofuranone and naphthofuran from hydroxy-naphthofuranone derivatives, which represents a unique addition to the field. Importantly, all reactions were carried out under gentle settings, without the use of harsh chemicals or high temperatures. The hypothesised mechanism is consistent with the observed substrate scope and control experiments. Notably, the process produces high yields of different hydroxy-naphthofuranone derivatives and has a wide tolerance for substituents. Our complete synthesis methodology shows great promise for effectively generating target molecules.

Conflicts of interest

There are no conflicts to declare.

Acknowledgements

S. R. sincerely thanks SERB, Government of India, New Delhi, for financial support under the SERB – Research Scientist Program (Grant No. SB/SRS/2022-23/78/CS) and thanks SASTRA Deemed University for Professor TRR research grant. V. H. gratefully acknowledges SASTRA Deemed University for the teaching assistantships. The authors gratefully acknowledge the DST-FIST grant (SR/FST/CS-I/2018/65) to SCBT, SASTRA Deemed University, for the NMR facility.

References

1 (*a*) P. Nimnual, K. Norseeda, B. Akkachairin, J. Tummatorn, P. Laohapaisan, N. Supantanapong, P. Chuangsoongnern, C. Thongsornkleeb, S. Sittihan, S. Ruchirawat and W. Rodphon, *Asian J. Org. Chem.*, 2018, **7**, 932–945; (*b*) M. Miura, T. Tsuda, T. Satoh and M. Nomura, *Chem. Lett.*, 1997, **26**, 1103–1104; (*c*) H. He, C. Qi, X. Hu, L. Ouyang, W. Xiong and H. Jiang, *J. Org. Chem.*, 2015, **80**, 4957–4965; (*d*) A. R. Gomez, R. O. Torres-Ochoa, R. Gamez-Montano, Q. Wang and J. Zhu, *Org. Lett.*, 2020, **22**, 7030–7033.

2 V. K. Omanakuttan, J. John and H. Hopf, *Eur. J. Org. Chem.*, 2020, **2021**, 163–201.

3 (*a*) V. Srivastava, A. S. Negi, J. K. Kumar, U. Faridi, B. S. Sisodia, M. P. Darokar, S. Luqman and S. P. S. Khanuja, *Bioorg. Med. Chem. Lett.*, 2006, **16**, 911–914; (*b*) V. E. Borisenko, S. A. Krekov, M. Yu. Fomenko, A. Koll and P. Lipkovski, *J. Mol. Struct.*, 2008, **882**, 9–23; (*c*) J. Padwal, W. Lewis and C. J. Moody, *J. Org. Chem.*, 2011, **76**, 8082–8087; (*d*) J. Maenpaa, R. Juvonen, H. Raunio, A. Rautio and O. Pelkonen, *Biochem. Pharmacol.*, 1994, **48**, 1363–1369; (*e*) P. J. Jerris and A. B. Smith, *J. Org. Chem.*, 1981, **46**, 577–585; (*f*) J. McK. R. Woollard, N. B. Perry, R. T. Weavers and J. W. van Klink, *Phytochemistry*, 2008, **69**, 1313–1318; (*g*) Q. Shou, L. K. Banbury, D. E. Renshaw, J. E. Smith, X. He, A. Dowell, H. J. Griesser, M. Heinrich and H. Wohlmuth, *J. Nat. Prod.*, 2013, **76**, 1384–1387; (*h*) D. M. Hodgson, D. Angrish, S. P. Erickson, J. Kloesges and C. H. Lee, *Org. Lett.*, 2008, **10**, 5553–5556; (*i*) Y.-H. Kang, H. J. Lee, C. J. Lee and J.-S. Park, *Biomol. Ther.*, 2019, **27**, 503–513.

4 (*a*) M. Tian, Y. Peng and J. Zheng, *Drug Metab. Dispos.*, 2022, **50**(5), 655–670; (*b*) B. Z. Mahmoud, M. K. Adel, O. S. Moustafa and R. M. Zaki, *J. Chem. Res.*, 2006, **2006**, 748–752; (*c*) T. Dao-Huy, M. Haider, F. Glatz, M. Schnürch and M. D. Mihovilovic, *Eur. J. Org. Chem.*, 2014, 8119–8125.

5 A. Radadiya and A. Shah, *Eur. J. Org. Chem.*, 2015, **97**, 356–376.

6 V. Srivastava, A. S. Negi, J. K. Kumar, U. Faridi, B. S. Sisodia, M. P. Darokar, S. Luqman and S. P. S. Khanuja, *Bioorg. Med. Chem. Lett.*, 2006, **16**, 911–914.

7 (*a*) A. Kumar, G. Srivastava, S. Srivastava, S. Verma, A. S. Negi and A. Sharma, *J. Mol. Model*, 2017, **23**, 1–16; (*b*) D. Goyal, A. Kaur and B. Goyal, *J. Med. Chem.*, 2018, **13**, 1275–1299.

8 G. Cozza, S. Sarno, M. Ruzzene, C. Girardi, A. Orzeszko, Z. Kazimierczuk, G. Zagotto, E. Bonaiuto, M. Luisa and L. A. Pinna, *Biochim. Biophys. Acta*, 2013, **1834**, 1402–1409.

9 R. Le Guével, F. Oger, A. Lecorgne, Z. Dudasova, S. Chevance, A. Bondon, P. Barath, G. Simonneaux and G. Salbert, *Bioorg. Med. Chem. Lett.*, 2009, **17**, 7021–7030.

10 (*a*) P.-T. Phan, T.-T. Nguyen, H.-N. Nguyen, B.-K. Le, T. Vu, D. Tran and T.-A. Pham, *Molecules*, 2017, **22**, 687; (*b*) T. M. Kadayat, S. Banskota, P. Gurung, G. Bist, T. Bahadur, A. Shrestha, J.-A. Kim and E.-S. Lee, *Eur. J. Org. Chem.*, 2017, **137**, 575–597; (*c*) A. Baldisserotto, M. Demurtas, I. Lampronti, D. Moi, G. Balboni, S. Vertuani, S. Manfredini and V. Onnis, *Eur. J. Org. Chem.*, 2018, **156**, 118–125; (*d*) T. Wakabayashi, N. Tokunaga, K. Tokumaru, T. Ohra, N. Koyama, S. Hayashi, R. Yamada, M. Shirasaki, Y. Inui and T. Tsukamoto, *J. Med. Chem.*, 2016, **59**, 5109–5114.

11 N. Battini, S. Battula, R. Ranjith Kumar and Q. N. Ahmed, *Org. Lett.*, 2015, **17**, 2992–2995.

12 Q. Gao, X. Wu, S. Liu and A. Wu, *Org. Lett.*, 2014, **16**, 1732–1735.

13 T. Deng, H. Wang and C. Cai, *Eur. J. Org. Chem.*, 2015, **2015**, 1569–1574.

14 M.-Y. Chang, K.-T. Chen, Y.-T. Hsiao and S.-M. Chen, *J. Org. Chem.*, 2020, **85**, 3605–3616.

15 (*a*) A. Bosveli, T. Montagnon, D. Kalaitzakis and G. Vassilikogiannakis, *Org. Biomol. Chem.*, 2021, **19**, 3303–3317; (*b*) T. C. Sherwood, H.-Y. Xiao, R. G. Bhaskar, E. M. Simmons, S. Zaretsky, M. Rauch, R. R. Knowles and

G. Murali, *J. Org. Chem.*, 2019, **84**, 8360–8379; (*c*) W. H. García-Santos, J. Ordóñez-Hernández, M. Farfán-Paredes, H. M. Castro-Cruz, N. A. Macías-Ruvalcaba, N. Farfán and A. Cordero-Vargas, *J. Org. Chem.*, 2021, **86**, 16315–16326; (*d*) T. C. Sherwood, N. Li, A. N. Yazdani and G. Murali, *J. Org. Chem.*, 2018, **83**, 3000–3012; (*e*) R. Saritha, S. Babiola Annes and S. Ramesh, *RSC Adv.*, 2021, **11**, 14079–14084.

16 (*a*) V. Kameshwara Rao, G. M. Shelke, R. Tiwari, K. Parang and A. Kumar, *Org. Lett.*, 2013, **15**, 2190–2193; (*b*) C. Sreenivasulu, K. Reddy and G. Satyanarayana, *Org. Chem. Front.*, 2017, **4**, 972–977; (*c*) B. Wang, Q. Zhang, J. Luo, Z. Gan, W. Jiang and Q. Tang, *Molecules*, 2019, **24**, 2187; (*d*) Q. Zhang, J. Luo, B. Wang, X. Xiao, Z. Gan and Q. Tang, *Tetrahedron Lett.*, 2019, **60**, 1337–1340; (*e*) J. Huang, W. Wang, H.-Y. He, L. Jian, H.-Y. Fu, X.-L. Zheng, H. Chen and R.-X. Li, *J. Org. Chem.*, 2017, **82**, 2523–2534; (*f*) K. Nakanishi, T. Sasamori, K. Kuramochi, N. Tokitoh, T. Kawabata and K. Tsubaki, *J. Org. Chem.*, 2014, **79**, 2625–2631; (*g*) N. Chalotra, I. H. Shah, S. Raheem, M. Ahmad Rizvi and B. Ali Shah, *J. Org. Chem.*, 2021, **86**, 16770–16784; (*h*) S. W. Youn and J. I. Eom, *Org. Lett.*, 2005, **7**, 3355–3358.

17 (*a*) C. Moldoveanu, I. Mangalagiu, D. L. Isac, A. Airinei and G. Zbancioc, *Molecules*, 2018, **23**, 1968–1968; (*b*) Q. Chen, P. Jiang, M. Guo and J. Yang, *Molecules*, 2018, **23**, 2450.

18 (*a*) D. G. Ho, R. Gao, J. Celaje, H.-Y. Chung and M. Selke, *Science*, 2003, **302**, 259–262; (*b*) Y. Zhang, C. Ye, S. Li, A. Adam Ding, G. Gu and H. Guo, *RSC Adv.*, 2017, **7**, 13240–13243.

19 M. DeRosa, *Coord. Chem. Rev.*, 2002, **233–234**, 351–371.

20 (i) The CCDC number for **10a** = 2350169; unit cell parameters: (a) 10.989(7), (b) 11.463(8), (c) 17.763(13), space group $P\bar{1}$. (ii) The CCDC number for **21a** = 2350170; unit cell parameters: (a) 8.7791(11), (b) 24.495(3), (c) 13.0852 (17), space group $P21/c$. (iii) The CCDC number for **14g** = 2360763; unit cell parameters: (a) 8.0311(5), (b) 10.4014(6), (c) 11.3139 (7), space group $P21$.

